Monoanionic Quasi-Imido Ligands Based on 1-Methyl-4-Iminopyridine and Complexes with the Main Group Elements Mg, Al and Zn.

Volodymyr Semeniuchenko, Samuel A. Johnson*

Department of Chemistry and Biochemistry, University of Windsor, Sunset Avenue 401, Windsor, ON, N9B 3P4, (Canada)

Fax: (+1) 519-973-7098

E-mail: sjohnson@uwindsor.ca

Abstract: The synthesis of a new class monoanionic nitrogen donor ligands based on (1-methylpyridin-4(1H)-ylidene)amide, abbreviated MQI (monoanionic quasi imide) and it chemistry with main group elements is reported. The electronic structure of the ligand allows delocalization of positive charge onto the N-heterocycle, which is accompanied by aromatization. The unsubstituted MQI ligand was found to form insoluble intractable products on reaction with non-transition metal alkyls, thus substituents were introduced to increase solubility and stability of those complexes and enable their study. The precursors 3,5-bis(3,5-dimethylphenyl)-1-methylpyridin-4(1H)-imine [MQI^{Me}]H and 3,5-bis(3,5-di-tert-butylphenyl)-1-methylpyridin-4(1H)-imine [MQI^{tBu}]H both gave isolable complexes. The species {[MQI^{tBu}]MgCl(THF)}$_2$, {[MQI^{tBu}]MgMe}$_2$, {[MQI^{tBu}]AlMe$_2$}$_2$, {[MQI^{tBu}]ZnMe}$_2$, and {[MQI^{Me}]MgCl(THF)}$_2$ were prepared. As well, [MQI]H precursors were coordinated with Lewis acidic boron- and aluminium-derived Lewis acids. Charge delocalization onto pyridine was examined by crystallography and NMR spectroscopy.

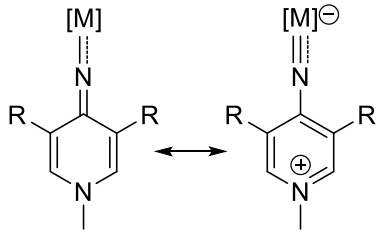

[MQI]M

M = Mg, Al, Zn

MQI: a Monoanionic quasi-imido donor capable of delocalization of positive charge onto ligand

Introduction.

Anionic amido ligands ($RR'N^-$) are the quintessential π-donor ligand for the stabilization of early transition metals,[1] lanthanides[2, 3] and actinides[4] in high oxidation states. Their stabilizing influence has made amido moieties commonly featured in spectator ligand designs for both stoichiometric and catalytic reactions.[5, 6] Structurally-related ligands that possess terminal monoanionic nitrogen atoms such as ketimido, $R_3P{=}N^-$,[7-9] and more recently $R_2C{=}N^-$[10-15] have all garnered interest, and often viewed as isoelectronic to the ubiquitous cyclopentadienyl ligand. Complexes of these related ligands type have found application in catalytic intramolecular alkene hydroamination,[3] intermolecular alkene hydrosilylation,[2, 3] alkyne metathesis,[16] reductive desulfurisation of dibenzothiophene,[17] and polymerization of ethylene[18] and ε-caprolactone.[19] Selected anionic nitrogen donors and their charges and σ- and π-donation properties are given in Scheme 1. In some cases, resonance structures can be drawn that suggest a delocalization a positive charge from metal to ligand atoms other than the coordinated nitrogen.[3, 20, 21]

Ligand Name	Structure	Charge	Donation
amide		–1	$2\sigma, 2\pi$
imide		–2	$2\sigma, 4\pi$
ketimide	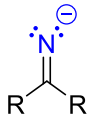	–1	$2\sigma, 2\pi$
phosphinimide (phosphorane imidate)	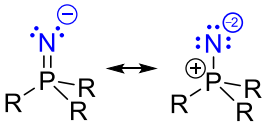	–1	$2\sigma, 4\pi$
imidazolin-2-iminate	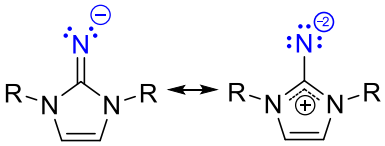	–1	$2\sigma, 4\pi$

Scheme 1. Selected anionic nitrogen donors and their charges and σ- and π-donation properties, including resonance structures that delocalize positive charge onto the ligand.

Our group has previously reported the synthesis of a neutral quasi-amido ligand $MeNC_5H_4N^iPr$, with conventional name *N*-(1-isopropyl**p**yridin-4(1*H*)-**y**lid**e**ne)amine (PYE), abbreviated [NQA] herein, and explored its chemistry in C–F and C–H bond activation, as shown in Scheme 2.[22-25] The [NQA] ligand can be represented by two resonance structures, shown on the left of Scheme 2A. The first resonance structure avoids charge separation but lacks aromaticity. The second resonance structure is zwitterionic with an anionic amide. This structure has the disadvantage of charge separation, but maintains aromaticity. This combination of resonance structures is reminiscent of the resonance structures of N-heterocyclic carbene (NHC) ligands, suggestive that the [NQA] ligand might behave as a hard N-donor NHC analogue. Despite a solid-state structure with bond lengths suggestive of the non-zwitterionic form, [NQA] is a strong base in aqueous solution. The donor properties based on the $[NQA]Rh(CO)_2Cl$ ν_{CO} stretching frequency are comparable to that of NHC ligands, as shown on the right side of Scheme 2A.[23] The [NQA] ligand has been shown to mediate Ni(0) C-F bond activation,[23] as shown in Scheme 2B, and

has also been used as an ancillary ligand in an unprecedented C-H bond functionalization, to give new C-Sn bonds using $H_2C{=}CHSnBu_3$,[22, 24, 25] as shown in Scheme 2C. Despite the hard nature of the [NQA] donor, it has been shown to support both Ni(II) and Ni(0) complexes.[23]

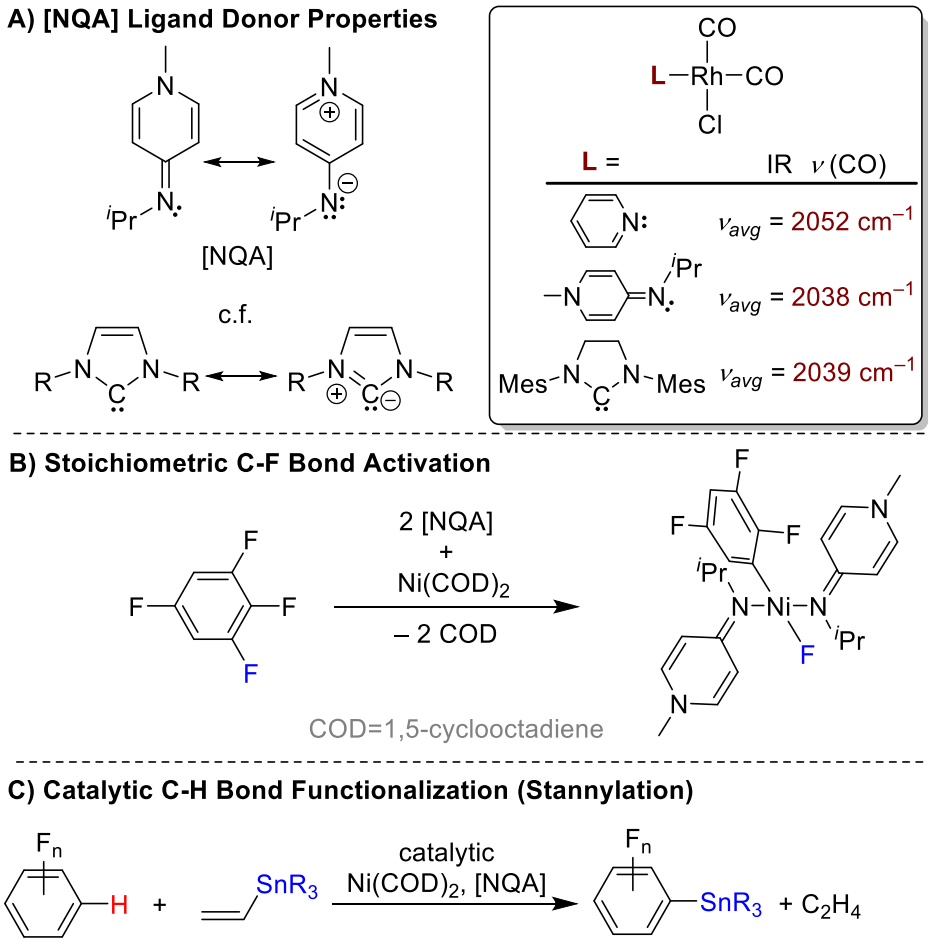

Scheme 2. Previous work on the NQA ligand's donor properties and use as an ancillary ligand in stoichiometric C-F activation and catalytic C-H functionalization.

The Douthwaite group has thoroughly explored coordination chemistry of the related donor N-(1-alkylpyridin-**2(1H)**-ylidene)amine,[26] and has discovered its Ru-complex application as sensitizer for solar cells[27] Despite high structural and electronic similarity between N-(1-alkylpyridin-**2(1H)**-ylidene)amine and N-(1-alkylpyridin-**4(1H)**-ylidene)amine, their coordination chemistry might be quite different, as was shown for related Ir-complexes.[28] A related neutral ligand, (1-isopropylpyridin-1-ium-3-yl)(phenyl)amide, having rigidly separated charges, was as well reported by this group.[29] A few publications report the use of PYE ligands in catalysis. Douthwaite et al. have shown that Pd(PYE) is analogous to Pd(NHC), and then Munir et al.[30] reported Pd(PYE)-catalyzed Heck–Mizoroki cross coupling. Separation of charges allowed the modulate of catalytic activity in Ru complexes by changing the solvent polarity: both catalytic oxidation[31, 32] and reduction[32] were dependent on polar cosolvent. In addition the Albrecht group has communicated the use of 0.1 ppm of Ru(PYE) complex as a catalyst for the oxidative cleavage of alkenes[33] and catalytic transfer hydrogenation,[34] Ir(PYE) for catalytic transfer hydrogenation and hydrosilylation,[35] and water oxidation.[36, 37]

In this article we describe the design and synthesis of the negatively charged analogue of [NQA], a monoanionic quasi-imido ligand, [MQI], shown in Scheme 3, from deprotonation of 4-pyridonimines (4(1*H*)-pyridinimines). The [MQI] ligand is anticipated to be an excellent donor for metals that would be

stabilized by the aromatization of pyridine ring in [MQI]. This resonance form provides means to increase electron donation on the metal centre, because the [MQI] would behave as a 6-electron donor. Charge separation from this resonance form was anticipated to have the negative effect of poor complex solubility in nonpolar solvents; however this should be mitigated by incorporating nonpolar functional groups. Groups in the ortho-positions to the N donor are also likely to provide kinetic stabilization of metal complexes; synthetic approaches to this are developed in this work. The application of these ligands to make main group precursors for further transmetallation reactions are demonstrated, and the ligands potential to stabilize charge separation is examined.

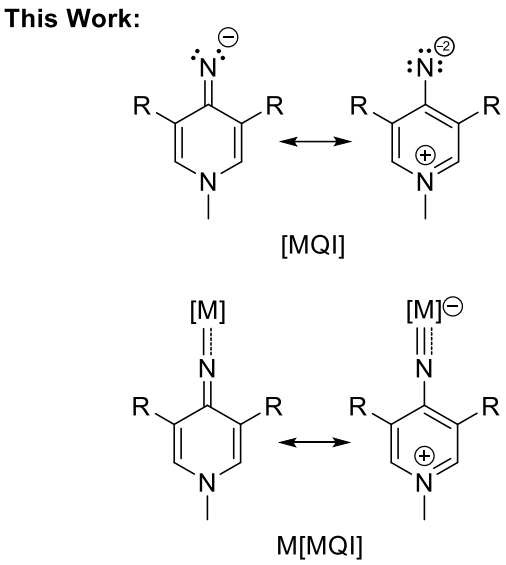

Scheme 3. Monoanionic Quasi-Imine [MQI] ligands targeted in this study.

Results and discussion.

The unfunctionalized species **1** (where R = H in Scheme 3) was first communicated in 1925,[38, 39] but no use of this species as a ligand has been reported. Previous preparations used water, and great effort was taken to separate the product; we found that **1** could be prepared in excellent yield from 1-methyl-4-aminopyridinium iodide (**1·HI**) in reaction with NaH using catalytic amounts of NaO^tBu, as shown in Scheme 4. This reaction yielded the adduct **1**·NaI, which is soluble only in highly polar solvents like DMF and DMSO, but rapid sublimation at 300 °C efficiently liberated salt free **1**. Compound **1** was fully characterized by NMR, HRMS and single crystal x-ray diffraction. In solid state compound **1** has dimeric structure: two independent molecules are linked by hydrogen bond, as shown in Figure 1The ^1H NMR spectrum of **1** show sharp peaks consistent with rapid exchange of the pairs of ortho 2-CH/6-CH and meta 3-CH/5-CH sites at room temperature, indicative of a rapid fluctional process involving the NH bond orientation, as shown in Scheme 4.

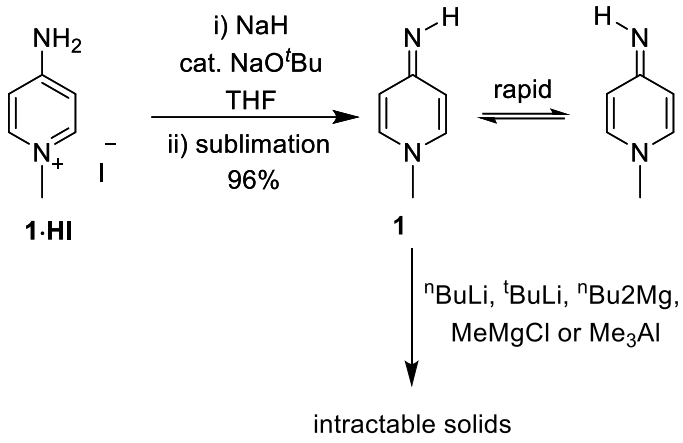

Scheme 4. New synthetic route to 1 and attempted reaction with main group metal alkyls.

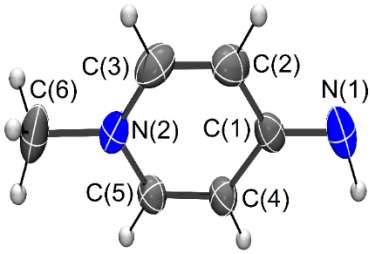

Figure 1. ORTEP depiction of one of two molecules of **1** in the asymmetric unit, as determined by single-crystal X-ray crystallography.

It should be noted that the first report of **1** in 1925[38, 39] gave minimal supporting characterization beyond its melting point of 150-151 °C. Since then **1** has had many reported alternate syntheses,[40] properties[40-48] and applications,[49-52] and is currently commercially available. To the best of our knowledge the solid-state structure of **1** has not been previously reported and the only reported ^{1}H NMR data appears incorrect,[46] since it matches the spectrum we observe for the precursor cation **1·H$^+$**, not **1**. About compound **1,** S.J. Angyal and C.L. Angyal[40] wrote "because of its extreme sensitivity to oxygen, carbon dioxide, and water, however, it seemed unsuitable for purification, analysis and weighing". Although this suggested that perhaps the syntheses of **1** from 1925 reported were possibly a hydrate, there is ^{13}C{^{1}H} and ^{15}N NMR spectroscopic evidence reported by Stefaniak,[45] which match those obtained by us for **1**; these confirm that it is possible to obtain **1** via previous literature syntheses, though the improved method we describe here provides near quantitative yield and eliminates the need to remove water in the last step. The previous literature never reported yields of **1** and so they cannot be compared. As might be expected, compound **1** reacts rapidly with the main group metal alkyls ^{n}BuLi, ^{t}BuLi, ^{n}Bu$_2$Mg, MeMgCl and Me$_3$Al, but gives intractable solids, as shown in the bottom of Scheme 4. These solids were insoluble in common organic solvents (THF, Et$_2$O) and unstable in highly polar ones (DMF, DMSO, MeCN, Py, CHCl$_3$ and CH$_2$Cl$_2$), which was not unexpected.

To address the issue of solubility after deprotonation and coordination using **1**, we designed its functionalized analogues [MQI^{Me}]H (**2**) and [MQI^{tBu}]H (**3**) as shown in Scheme 5. The crucial stage in the syntheses is the installation of the functional groups by Pd(PPh$_3$)$_4$ catalyzed Suzuki-Miyaura coupling of an arylboronic acid with 3,5-dibromo-4-aminopyridine to yield compounds **4** and **5**. This reaction type

was first reported in the patent literature[53] with small loads of reagents and chromatographic purification of the product. For the large scale synthesis of these ligands, it proved worthwhile to optimize the coupling reactions to maximize yield and eliminate the need for chromatography. Details of this optimization are given in the Supporting Information. Compounds **4** and **5** were methylated by MeI to give the 1-methylpyridinium salts $[MQI^{Me}]H_2^+I^-$ (**6**) and $[MQI^{tBu}]H_2^+I^-$ (**7**), which were treated with excess NaH to yield the ligand precursors $[MQI^{Me}]H$ and $[MQI^{tBu}]H$ in near quantitative yields.

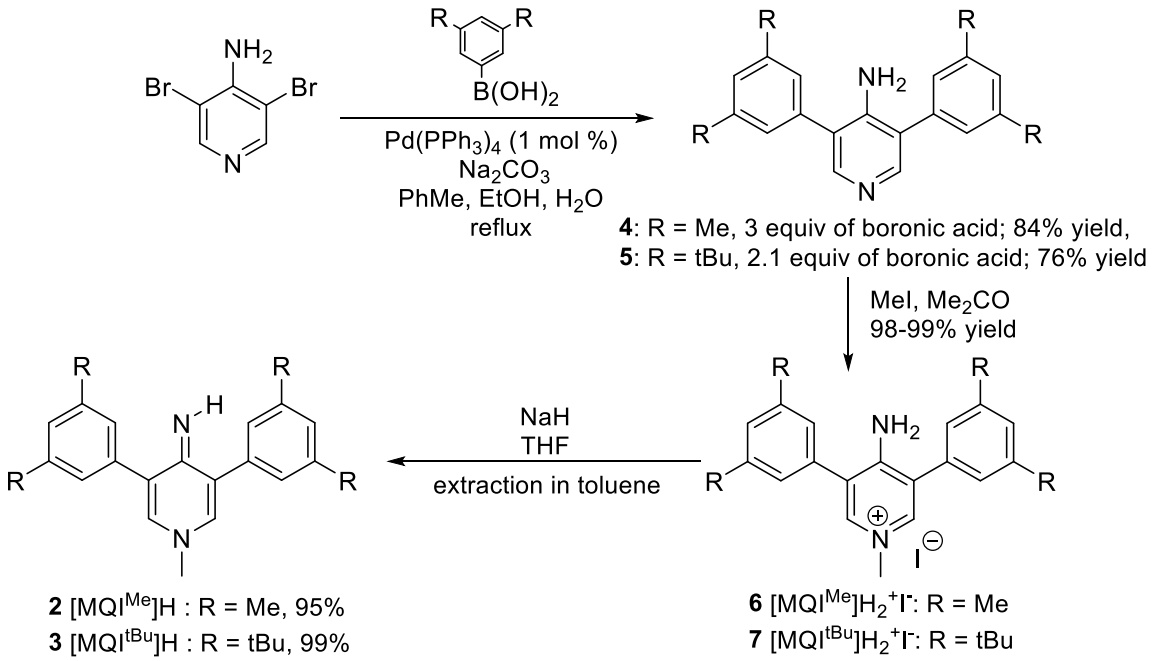

Scheme 5. Synthesis of 2 and 3

Attempts were made to obtain single crystals suitable for X-ray diffraction for the pyridinium salts $[MQI^{Me}]H_2^+I^-$ (**6**) and $[MQI^{tBu}]H_2^+I^-$ (**7**) by various methods, but failed to provide samples suitable for crystallographic experiments. Using the chloride anion allowed for the crystallization of $[MQI^{tBu}]H_2^+Cl^-$ (**8**) and its solid-state structure was determined with a solvated methanol hydrogen bonded to the NH_2 moiety. An ORTEP depiction of **8** is shown in Figure 2.

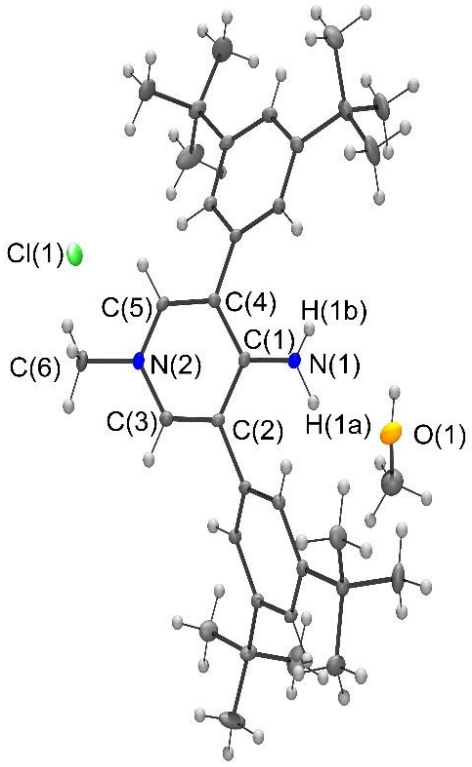

Figure 2. ORTEP depiction of $[MQI^{tBu}]H_2^+Cl^-$(**8**), with a solvated methanol, as determined by single-crystal X-ray crystallography.

The compounds $[MQI^{Me}]H$ (**2**) and $[MQI^{tBu}]H$ (**3**) were both characterized by single crystal X-ray diffraction. An ORTEP depiction for each is shown in Figure 3. Unlike compound **1**, they adopt monomeric structure and do not display intermolecular hydrogen bonding.

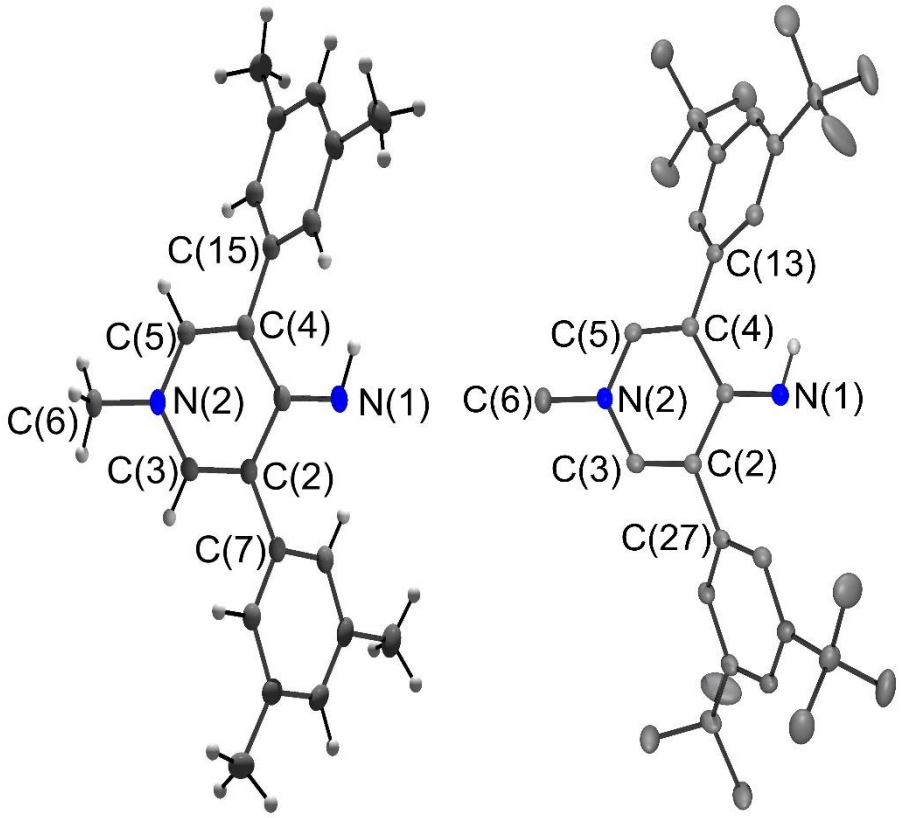

Figure 3. ORTEP depictions of [MQI^{Me}]H (**2**, left) and [MQI^{tBu}]H (**3**, right) as determined by single-crystal X-ray crystallography. For [MQI^{tBu}]H only the N-H hydrogen is shown, with the remaining hydrogens omitted for clarity.

The compounds [MQI^{Me}]H (**2**) and [MQI^{tBu}]H (**3**) were characterized by NMR spectroscopy in various solvents. Broad signals were observed in the ^{1}H NMR of both compounds in a number of solvents, however addition of even trace quantities (1 mol%) of KH or any other strong base (LiH, NaH, LiHMDS, NaHMDS, Ti(NMe$_2$)$_4$, Y(HMDS)$_3$) directly to NMR tube changed the spectra to show very sharp peaks, consistent with a C_s symmetric species. In the absence of strong base some acid efficiently catalyzed proton flip at 4-N, as shown in Scheme 6, thus equilibrating aryl groups and 2-CH/6-CH protons and carbons. In Teflon NMR tubes the same broadening was observed, thus protonation of [MQI^{Me}]H and [MQI^{tBu}]H by surface OH-groups on glass cannot be the only cause. It should be noted that **1**, **2** and **3** all decomposed in CH_2Cl_2, MeCN and DMSO over a few hours, forming pyridinium salts.

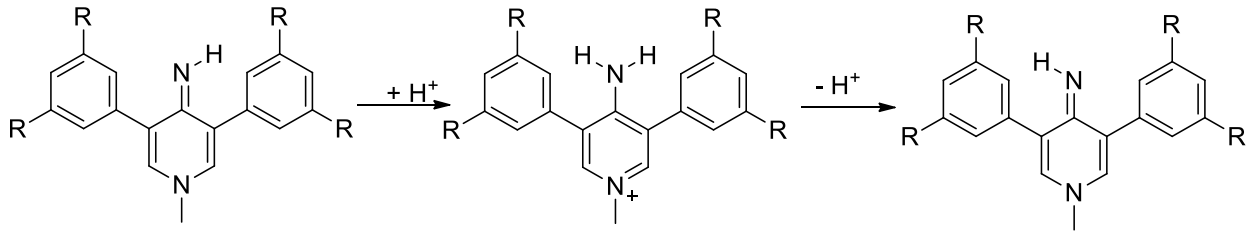

Scheme 6. Proton catalysed dynamic NMR exchange in [MQI^{Me}]H (left) and [MQI^{tBu}]H.

The compounds [MQI^{Me}]H and [MQI^{tBu}]H react immediately with Lewis acids such as AlMe$_3$ and B(C$_6$F$_5$)$_3$, as shown in Scheme 7. The reaction with AlMe$_3$ at room temperature gave quantitative

formation of the corresponding adducts. The compounds [MQI^{Me}]H·AlMe$_3$ (**9**) and [MQI^{tBu}]H·AlMe$_3$ (**10**) were characterized by multinuclear NMR spectroscopy, but required heating to undergo further elimination of methane (vide infra). The reaction of [MQI^{Me}]H with B(C$_6$F$_5$)$_3$ allowed us to observe adduct [MQI^{Me}]H·B(C$_6$F$_5$)$_3$ (**11**) by NMR in C$_6$D$_6$; it was crystallized from toluene, but pure crystalline compound **11** has lost solubility in organic solvents, and was not suitable for characterization in solution.

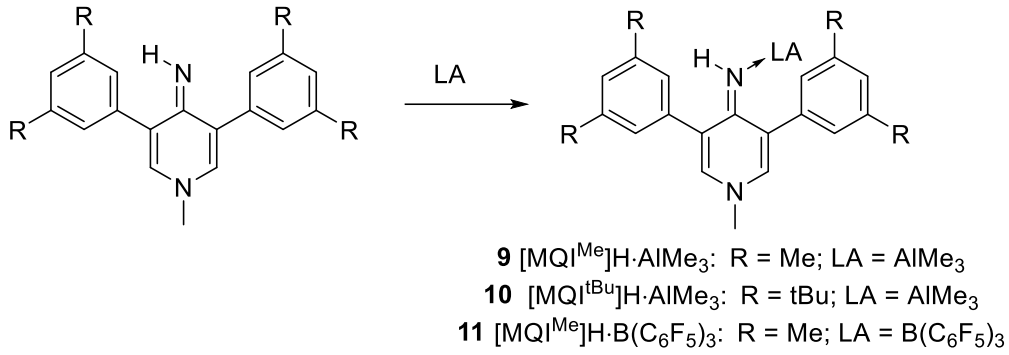

9 [MQI^{Me}]H·AlMe$_3$: R = Me; LA = AlMe$_3$
10 [MQI^{tBu}]H·AlMe$_3$: R = tBu; LA = AlMe$_3$
11 [MQI^{Me}]H·B(C$_6$F$_5$)$_3$: R = Me; LA = B(C$_6$F$_5$)$_3$

Scheme7. Reactions of [MQI]H with Lewis acids.

An ORTEP depiction of [MQI^{Me}]H·B(C$_6$F$_5$)$_3$ (**11**) is shown in Figure 4. Steric congestion between the 2-H moiety and B(C$_6$F$_5$)$_3$ is suggested by the C(1)-N(1)-B(1) angle of 140.4(2) °, which is significantly larger than expected for an sp^2 hybridized N. The B(C$_6$F$_5$)$_3$ moiety also appears to be accommodated by a distortion at C(1), with unequal N(1)-C(1)-C(2) and N(1)-C(1)-C(4) angles of 127.7(2) versus 116.8(2) °. Consistent with the proposed strain in [MQI^{Me}]H·B(C$_6$F$_5$)$_3$, the reaction of the larger [MQI^{tBu}]H with B(C$_6$F$_5$)$_3$ gave a complicated mixture, as observed by NMR spectroscopy, suggestive that the extra bulk of the [MQI^{tBu}]H ligand prevents the formation of a stable adduct.

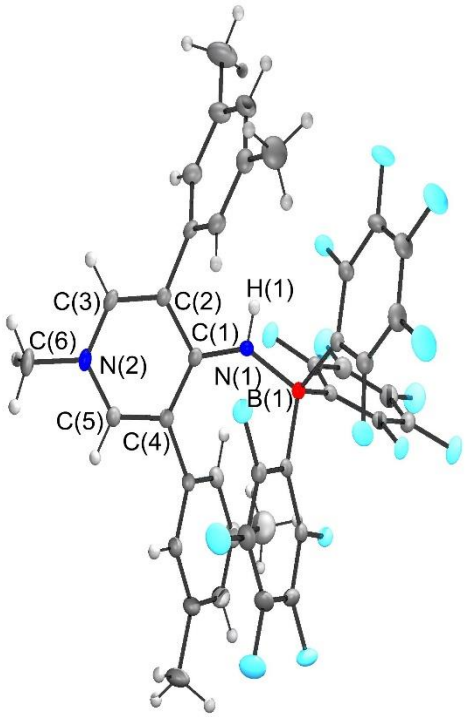

Figure 4. ORTEP depiction of [MQI^{Me}]H·B(C$_6$F$_5$)$_3$ (**11**).

We explored the reactions of the MQI-precursors with basic metal alkyls capable of deprotonating the NH moiety, as shown in Scheme 8. The reaction of one equivalent of [MQI^{tBu}]H (**3**) with MeMgCl·THF, Me$_2$Mg, Me$_3$Al and Me$_2$Zn yielding the corresponding compounds {[MQI^{tBu}]MgCl(THF)}$_2$ (**12**),

{[MQI^{tBu}]MgMe}$_2$ (**13**), {[MQI^{tBu}]AlMe$_2$}$_2$ (**14**) and {[MQI^{tBu}]ZnMe}$_2$ (**15**). All these compounds adopt a dimeric structure, as shown by single-crystal X-ray diffraction studies, with bridging MQI ligands. For different metal alkyls the necessary reaction conditions were significantly different. The reaction with Me_2Mg could be done at room temperature but the product **13** did not tolerate heating above 60 °C. the reaction with MeMgCl·THF was best done at 90 °C, and the product **12** did not tolerate heating to 120 °C. The complexes {[MQI^{tBu}]AlMe$_2$}$_2$ (**14**) and {[MQI^{tBu}]ZnMe}$_2$ (**15**) were formed only under the harsh conditions of 150 °C, for 1-3 days, and there was no decomposition observed. The methyl bearing compounds {[MQI^{tBu}]MgMe}$_2$ (**13**), {[MQI^{tBu}]AlMe$_2$}$_2$ (**14**) and {[MQI^{tBu}]ZnMe}$_2$ (**15**) failed to react with another equivalent of [MQI^{tBu}]H; no reaction occurred and on heating 50-150 °C in THF or toluene, other than decomposition in the case of **13**. The base NEt_3 was insufficient to break the MQI-bridge in **12**-**15** as judged by NMR spectroscopy, where no change of chemical shifts was observed. As well, dimeric {[MQI^{tBu}]MgMe}$_2$ (**13**) could be crystallized from a NEt_3-pentane solution.

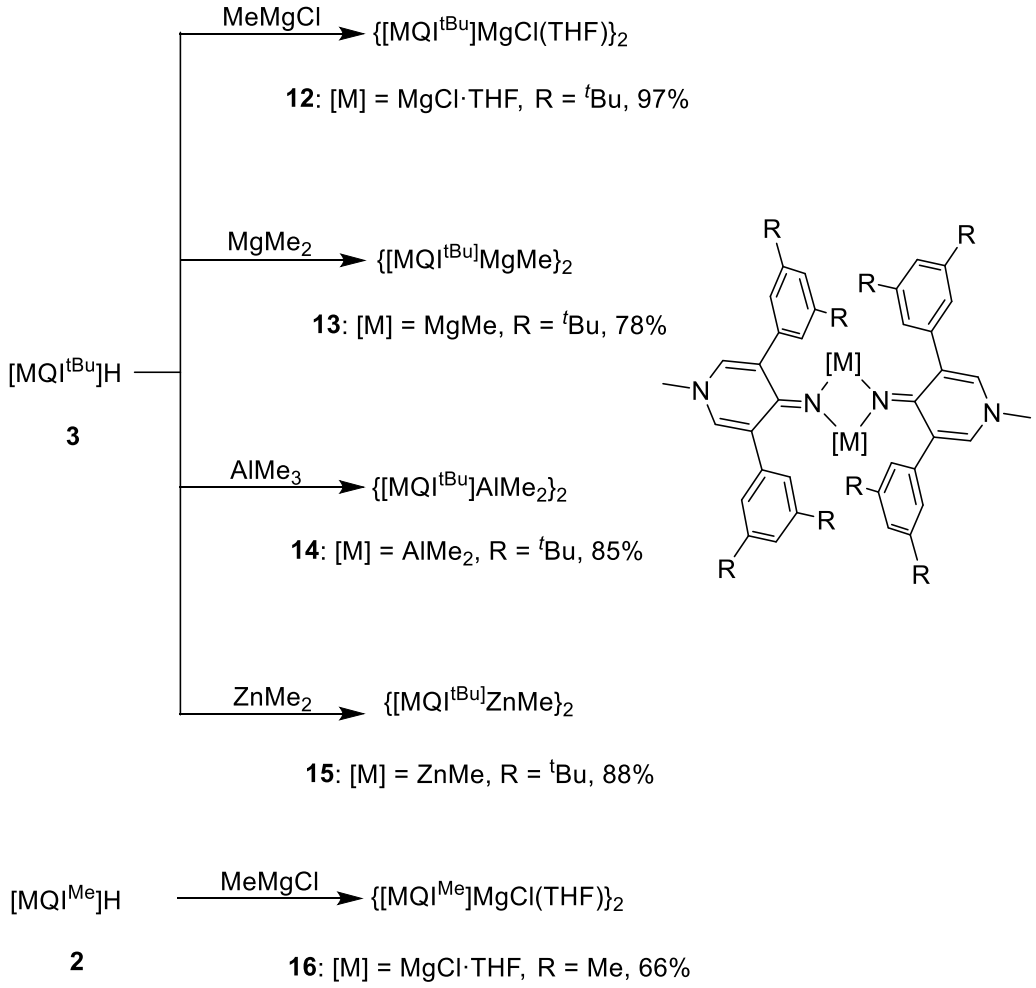

Scheme 8. Deprotonation and coordination of MQI ligand precursors **2** and **3** by main group alkyls.

In contrast, for the less bulky [MQI^{Me}]H (**2**) successful deprotonation only occurred using MeMgCl·THF (Scheme 7), but even in this case the reaction was problematic. The product {[MQI^{Me}]MgCl(THF)}$_2$ (**16**) was found to be unstable above 50 °C, thus the deprotonation was done at 40 °C. Under these conditions the reaction rate was very slow, and **16** was isolated with 66% yield after 4 days heating. Performing this reaction at room temperature for 2 weeks allowed for the isolation of single crystals of **16**, but its isolated yield was only 58%. Deprotonation of **2** by Me_3Al via the adduct **9** required elevated temperature, which led to ligand decomposition. Reactions of **2** with ^{n}BuLi, ^{t}BuLi, PhLi

and MeLi at room temperature were always accompanied by ligand decomposition, and on cooling (-30 °C and lower) the deprotonation rate was negligible. Pure complexes **12-16** could be quenched by addition of methanol, which recovered pure cations $[MQI]H_2^+$. For the cases where ligand decomposition was suspected, in the same manner crude reaction mixtures were quenched by addition of methanol, and then dioxane was added as internal standard. The latter allowed to quantify by NMR the amount of survived $[MQI]H_2^+$, and significant deviation from the quantity of initially introduced [MQI]H was a symptom of ligand decomposition (decomposition products remained intractable).

As already noted, compound $\{[MQI^{tBu}]MgCl(THF)\}_2$ (**12**) was prepared from MeMgCl·THF and **3** at 90 °C over 10 h with excellent yield. The conditions of deprotonation were obtained by following this reaction by variable-temperature ^1H NMR in a sealed J. Young tube with a Teflon seal. Mixing **3** with 1 equiv of MeMgCl in THF immediately changed the shift of MgMg group from δ –1.85 to δ –2.35 ppm, consistent with immediate coordination of MeMgCl onto Lewis basic imine group of **3**. On storage of this mixture at 25 °C, deprotonation was too slow to observe any amount of **12** in the ^1H NMR. Measuring NMR spectra at 60 °C every 30 min, conversion to **12** was calculated by integration of peaks at δ 8.59 (2-CH and 6-CH of **12**) and at δ 6.55 (2-CH of **3**). The process started from 20% conversion (0.5 h) and was stopped after 80 % conversion, which took 15 h. The observed rate suggests a 99.8% conversion is achievable within 40 hours. As a general rule, a 10 °C increase in temperature enhances reactions rates twofold, and indeed it was found that at 90 °C the reaction takes place over 10 h yielding **12**. At 120 °C decomposition of organic ligand was observed already in 1 h. Compound **12** is potentially the most valuable precursor to prepare organometallic complexes of $[MQI^{tBu}]$ with transition metals by transmetallation. The same utility also pertains to $\{[MQI^{Me}]MgCl(THF)\}_2$ (**16**) for the preparation of $[MQI^{Me}]$ complexes; however, the poor solubility of **16** in common solvents is anticipated to complicate transmetallation.

A surprising result of these studies was the difficulty of deprotonation of the N-H bonds in $[MQI^{Me}]H$ (**2**) and $[MQI^{tBu}]H$ (**3**) by capable strong bases. Compound **3** was combined with benzylpotassium in C_6D_6, but no reaction was observed up to 90 °C, and decomposition was observed upon heating at 110 °C. Both compounds **2** and **3** did not react with LiH, NaH, KH, $LiN(SiMe_3)_2$, $NaN(SiMe_3)_2$ or $Y[N(SiMe_3)_2]_3$ in refluxing toluene or THF. Under reflux in toluene with KH a slight decomposition of **2** was observed, while in all other cases **2** and **3** remained intact. Reaction of compounds **2** and **3** with $^nBu_2Mg$ occurred, but the nature of the products was unclear; they were insoluble in THF or less polar solvents and decomposed in other common organic solvents.

Solid-state structures for $\{[MQI^{Me}]MgCl(THF)\}_2$ (**16**) and $\{[MQI^{tBu}]MgCl(THF)\}_2$ (**12**) were obtained by single-crystal X-ray diffraction studies. ORTEP depictions are shown in Figure 4. Notable in both structures is the deviation of C(1)-C(5) and N(2) from the plane of the Mg_2N_2 core, so that the whole molecule adopts a chair like arrangement of the ligands with respect to the central core, easiest seen in the side-view of **16** on the bottom left of Figure 4. The aromatic functional groups are arranged to create a pocket to accommodate the central Mg, Cl and THF.

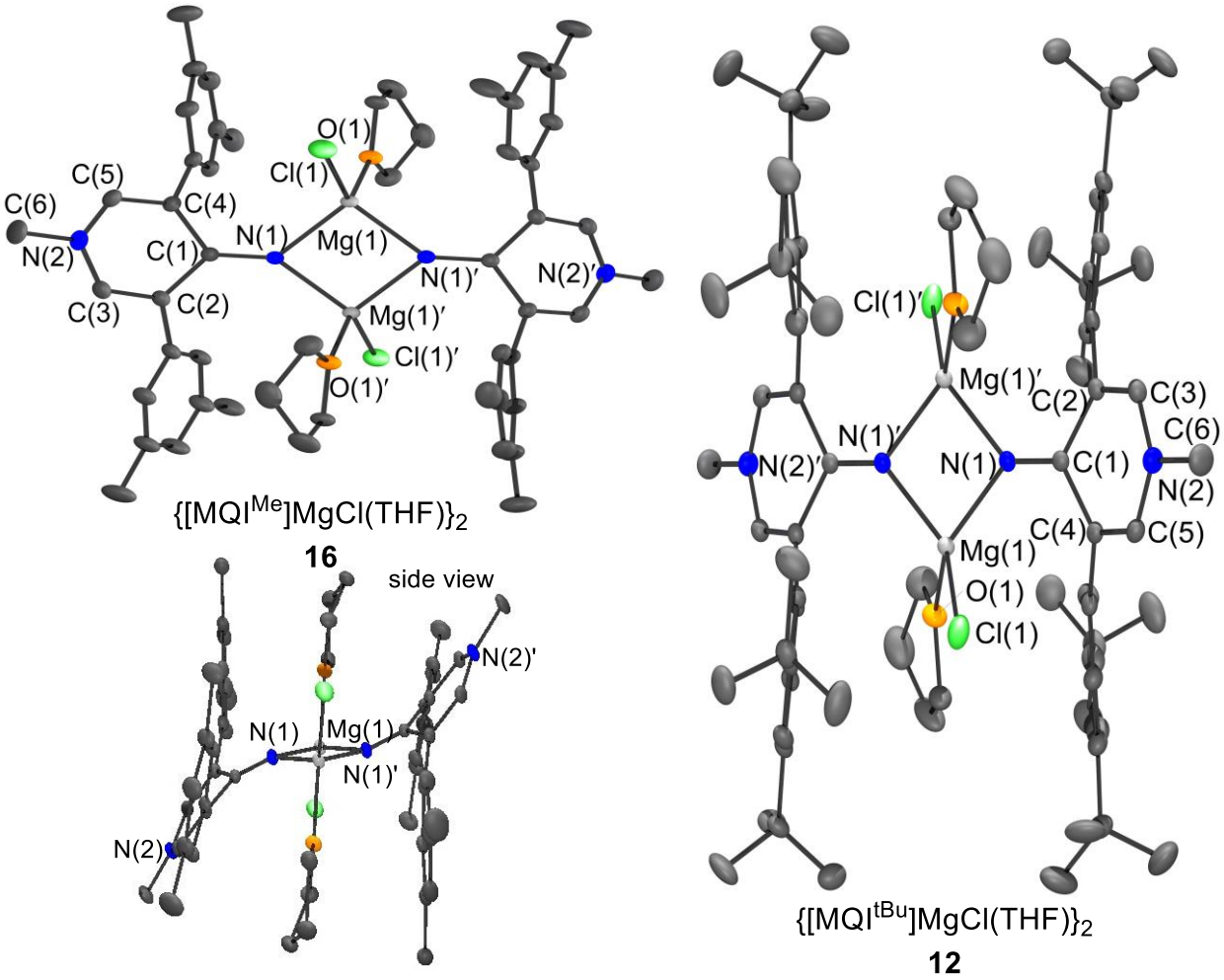

Figure 4. ORTEP depictions of $\{[MQI^{Me}]MgCl(THF)\}_2$ (**16**) and $\{[MQI^{tBu}]MgCl(THF)\}_2$ (**12**).

The solid-state structure of $\{[MQI^{tBu}]MgMe\}_2$ (**13**) is shown in Figure 5. Despite the apparent similarities with **12**, the structure of **13** features some notable differences. The Mg(1) and Mg(2) centres are three coordinate. The ligands adopt a boat-like conformation, as opposed to the chair-like conformation seen in **12** and **16**, where both MQI ligands are on the same side of the central Mg_2N_2 core. The boat-like structure of **13** also features a large twist of the MQI ligands along the N(1)-C(1) and N(3)-C(7) axes, a view of which is shown on the right of Figure 5. This twist likely aids in the minimization of steric interaction between the pair of MQI ligands in **13**, but does not appear electronically ideal given the fact that the pair on lone pairs on N(1) and N(3) should reside in the plane orthogonal to the N=C π-bond in the predominant resonance structure of the MQI ligand.

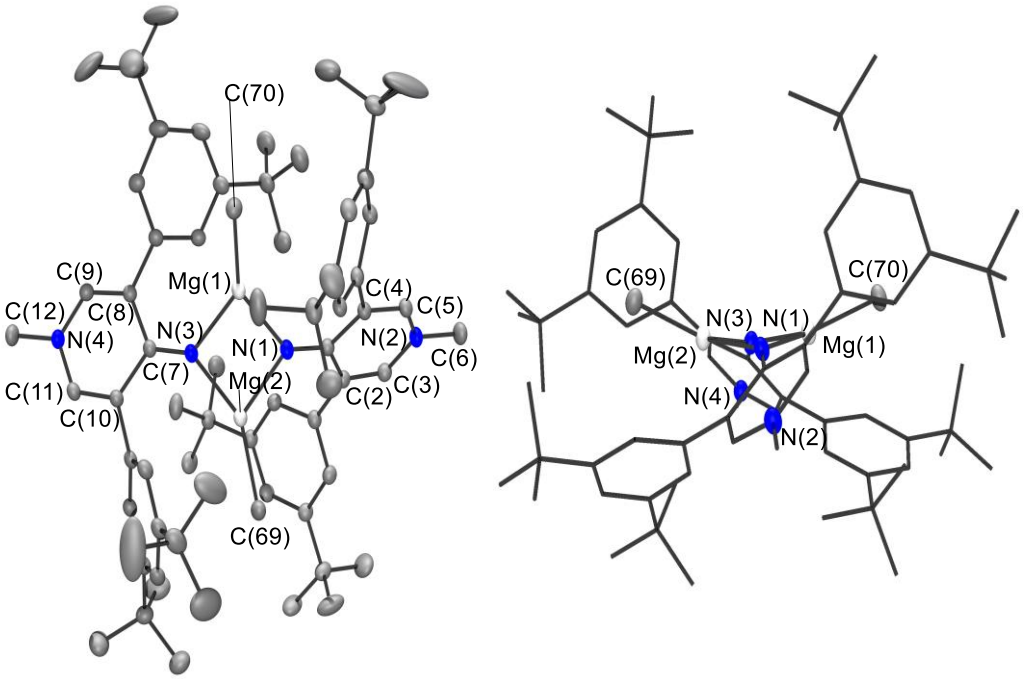

Figure 5. ORTEP depictions of {[MQI^{tBu}]MgMe}$_2$ (**13**), with hydrogens omitted for clarity. The second view of the molecule along the N(1)-N(3) axis (right) shows the boat-like conformation and the opposing twist of the MQI ligands along the N(1)-C(1) and N(3)-C(7) axes.

The solid-state structures for {[MQI^{tBu}]AlMe$_2$}$_2$ (**14**) and {[MQI^{tBu}]ZnMe}$_2$ (**15**) were also determined by X-ray crystallography, and ORTEP depictions are shown in Figure 6. Complex **14** features a chair-like conformation of the MQI ligands with respect to the Al$_2$ core, similar to **12**. Conversely, complex **15** features a boat-like conformation, with a twist of the MQI ligands, similar to that observed in structurally related **13**.

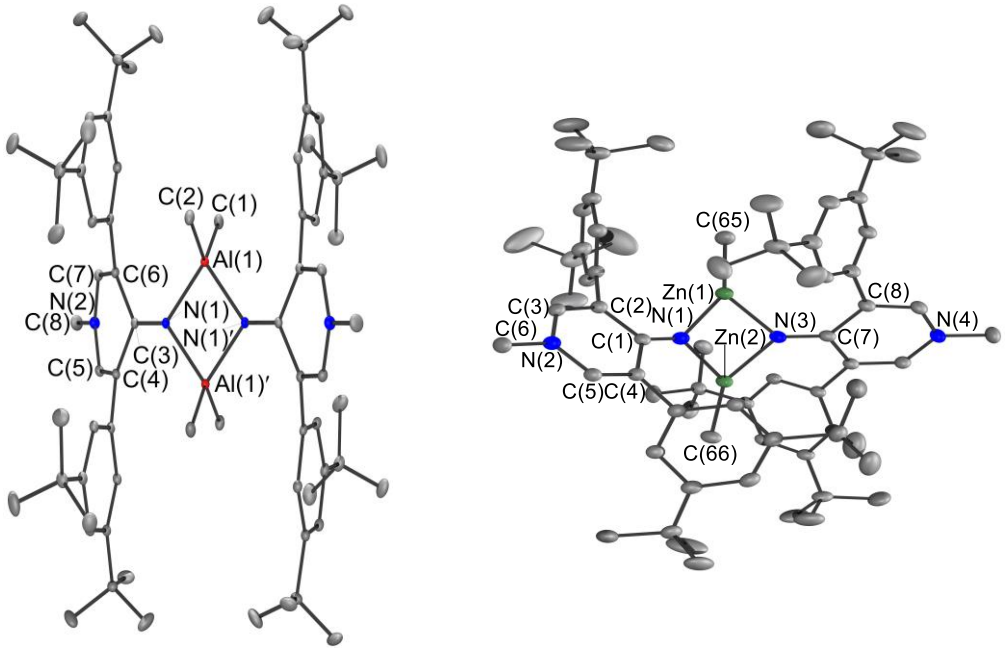

{[MQI^{tBu}]AlMe$_2$}$_2$ **14**

{[MQI^{tBu}]ZnMe}$_2$ **15**

Figure 6. ORTEP depictions of {[MQI^{tBu}]AlMe$_2$}$_2$ (**14**) and {[MQI^{tBu}]ZnMe}$_2$ (**15**), with hydrogens omitted for clarity.

All metal complexes reported here are very sensitive to water and other sources of reactive protons. Even halogenated aromatic compounds like polyfluorinated benzenes, PhF, PhCl, or CH_2Cl_2 react. Conversion of the methyl complex {[MQI^{tBu}]AlMe$_2$}$_2$ (**14**) to its chloride was attempted by reaction with 4 equiv of $NEt_3H^+Cl^-$ in THF or toluene. This instead gave quantitative formation of [MQI^{tBu}]$H_2^+Cl^-$ (**8**) along with Me_2AlCl; heating this mixture at 150 °C for 5.5 days gave no reaction, and both the Me_2AlCl and **8** remained intact, as shown in Scheme 9. The failure to deprotonate compound **8** is rationalized by reaction mechanism: weak Brønsted acid **8** reacts with Brønsted base NaH, but cannot coordinate Lewis acid Me_2AlCl.

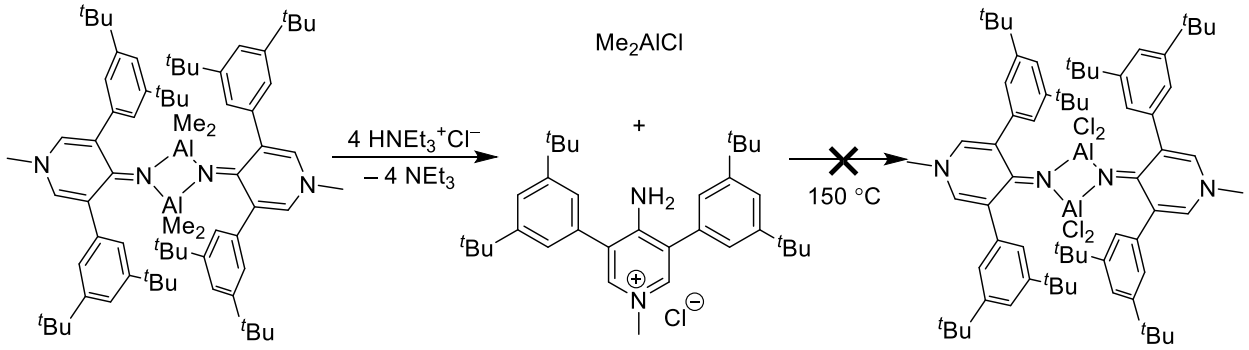

14 **8** Not observed

Scheme 9

Silylated complexes have potential use to install MQI ligands; related N-trimethylsililated ligands are often used in transmetallations with transition metal halides,[20] forming volatile Me_3SiCl as the only byproduct. Failed attempts to prepare the compounds [MQI^{Me}]$SiMe_3$ (**17**) and [MQI^{tBu}]$SiMe_3$ (**18**), are shown in Scheme 10. Compound **19** was smoothly prepared from lithium amide derived from compound **4** by the addition of Me_3SiCl. Precedent showed that the related reaction of the electrophilic

iodomethane with sodium pyridine-4-amide gave **1**, via 1-N-methylation rather than substitution at the amide nitrogen,[39] so the assignment of compound **19** was confirmed with the aid of ^{1}H-^{15}N HMBC spectra**.** The following cross-peaks were observed: 2-CH (^{1}H δ = 8.60) with 1-N (^{15}N δ = +289.0) and TMS (^{1}H δ = –0.30) with 4-NH (^{15}N δ = +65.2); in addition the latter signal had a weak correlation with NH proton (^{1}H δ = 3.68) visible as an artefact doublet (signals of this type should be suppressed in HMBC spectra, but the suppression is not always perfect, giving rise to characteristic artefact doublets). This confirms that compound **19** is 4-N-silylated, as shown in scheme 9. Unfortunately, methylation of compound **6** by MeI or MeOTf in various solvents always gave $[MQI^{Me}]H_2^+$, the cation of **6**, even with rigorous exclusion of contamination by moisture. Probably the methylation agent reacted not as electrophile, but rather as an acid; similar elimination of HI from iodomethane has been reported.[54] Attempts to silylate compounds **2** and **3** using 1 equiv of Me_3SiCl in THF or CH_2Cl_2 were not successful due to very slow reaction rate: instead THF was polymerized under action of Me_3SiCl or CH_2Cl_2 has protonated basic compounds **2** and **3**. A trial to accelerate silylation using excess of Me_3SiCl or $^{t}BuMe_2SiCl$ gave mixtures of mono- and bis-N-silylated compounds. Treatment of these mixture with NaH never gave NMR evidences of desired species **17-18** formation.

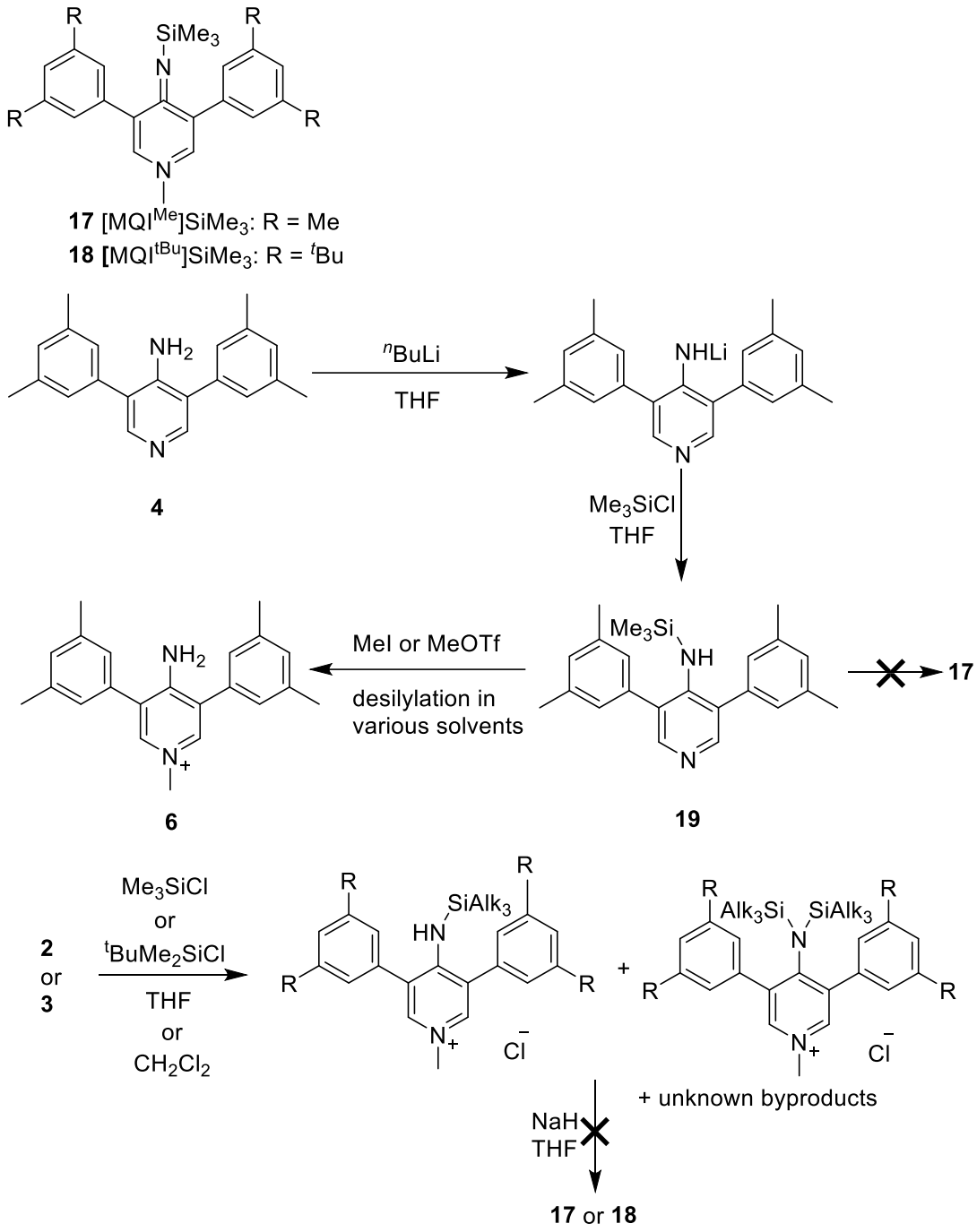

Scheme 10

A procedure of ligand precursor recovery was developed for **3**, to reuse it after unsuccessful attempts at coordination to various metals. Metal complex mixture with this ligand was quenched by MeOH, and then after evaporation of excess MeOH partitioned between CH_2Cl_2 and aqueous HCl. This gave nearly pure compound $[MQI^{tBu}]H_2^+Cl^-$ (**8**) in organic layer, which could be deprotonated by NaH in boiling THF. Quenching of metal complexes directly by CH_2Cl_2 always resulted in partial decomposition of organic part of ligand, thus it was not acceptable for recovery.

Charge separation is a useful feature of the MQI ligands, as shown in Scheme 3. This feature manifests itself as chemical shift changes in NMR spectroscopy. Charge separation is facilitated in polar solvents, and for the compounds reported a strong dependence of chemical shifts on solvents polarity, a measure of which is dielectric constant, was observed. NMR spectra were obtained in various solvents

for compound **2**, as shown in Table 1. There is a clear dependence of certain ^{1}H NMR chemical shifts on solvent polarity. Conversely, the ^{13}C NMR shifts do not show large variations correlating to solvent dielectric constant. By far the strongest correlation with solvent polarity is observed in the ^{15}N NMR, for the chemical shifts of the 1-NMe.

Table 1. Selected ^{1}H, ^{13}C and ^{15}N NMR chemical shifts for [MQI^{Me}]H (2) in a variety of solvents sorted by increasing dielectric constant.

Solvent	C_6D_6	C_6D_5Br	THF	CH_2Cl_2	CD_3CN	DMSO
dielectric constant	2.27	5.17	7.58	8.93	37.5	46.7
^{1}H NMR						
1-NMe	2.26	2.84	3.38	3.43	3.41	3.45
2-CH	6.16	6.37	6.83	6.75	6.88	7.08
4-NH	8.07	7.50			6.81	6.78
o-CH	7.38	7.20	7.13	7.02	7.07	7.10
m-Me	2.22	2.24	2.28	2.30	2.30	2.28
p-CH	6.84	6.80	6.87	6.92	6.95	6.93
^{13}C NMR						
1-NMe	41.18	41.65	42.10	42.77	42.72	41.55
2-CH	134.14	134.00	135.44	135.27	136.38	135.37
3-C	126.75	126.05	126.50	126.31	126.13	124.26
4-C	161.37	161.07	161.46	162.18	162.41	160.53
ipso-C	137.80	136.92	138.35	137.09	138.08	136.77
o-CH	127.73	127.12	127.82	127.21	127.81	126.68
m-C	137.77	137.34	137.92	138.43	138.84	136.97
m-Me	21.48	21.37	21.48	21.44	21.42	20.94
p-CH	129.17	128.86	129.07	129.32	129.59	128.28
^{15}N NMR						
1-NMe	112.8	114.1	114.4	116.1	118.5	119.9

A selection of ^{1}H, ^{13}C{^{1}H} and ^{15}N NMR chemical shifts for the key species reported in this work are summarized in Table 2. The pyridinium cations such as **1·HI**, [MQI^{Me}]H$_2^+$I$^-$ (**6**) and [MQI^{tBu}]H$_2^+$I$^-$ (**7**) are characterized by ^{13}C{^{1}H} NMR spectra with relatively shielded C-4 and unshielded 2-*C*H/6-*C*H relative to the **1**, **2** and **3**. The change of ^{1}H NMR chemical shifts NMe and 2-CH/6-CH correlate very well with solvent polarity, but otherwise is not diagnostic for pyridinium salts, pyridin-4(1H)-imines and N-metal complexes. The ^{15}N NMR chemical shift of the NMe group turned out to be an excellent reporter of the charge on pyridinium ring: in pyridinium salts it is always circa 160 ppm, and in neutral pyridin-4(1H)-imines in the range of 111-119 ppm. As well, the ^{15}N chemical shift showed good correlation with solvent polarity, because even a neutral pyridin-4(1H)-imine may be represented by a zwitterionic form in polar solvent. The ^{15}N NMe chemical shifts of [MQI^{Me}]H·AlMe$_3$ (**9**) (δ 146.9), [MQI^{tBu}]H·AlMe$_3$ (**10**) (δ 153.1) and [MQI^{Me}]H·B(C$_6$F$_5$)$_3$ (**11**) (δ 145.5) suggests that these compounds are best represented by the zwitterionic structure, with a positive charge on pyridine ring and negative charge on the Al or B. Alkyl-aluminium compounds are competent Lewis acids, and the bridging character of compound {[MQI^{tBu}]AlMe$_2$}$_2$ **14** can be described as coordination of Lewis acidic Al; the ^{15}N NMR NMe shift of 122.4 is the largest seen in the metal complexes studied in this work, and suggests a significant though not complete contribution by the zwitterionic resonance structure.

Table 2. Summary of select ^{1}H, ^{13}C and ^{15}N NMR chemical shifts.

Compd.	Solvent	Dielectric constant	^{1}H, δ			^{13}C, δ		^{15}N , δ
			NMe	2-CH/6-CH	NH	2-CH/6-CH	4-CN	NMe
1·HI	DMSO-d_6	46.7	2.51	6.74	7.86	144.4	159.1	157.9
1	DMSO-d_6	46.7	3.31	5.74	6.39	137.3	162.8	117.8
1	CD_3CN	37.5	3.29	5.79	6.34	138.1	164.6	
1	CH_2Cl_2	8.93	3.31	5.87	6.40	137.0	164.1	117.7
1	THF	7.58	3.29	5.72	6.47	136.3	163.4	
1	C_6D_6	2.27	2.10	5.66	7.08	135.9	163.3	111.8
$[MQI^{Me}]H$ (**2**)	DMSO-d_6	46.7	3.45	7.08	6.78	135.4	160.5	119.9
$[MQI^{Me}]H$ (**2**)	CD_3CN	37.5	3.41	6.88	6.81	136.4	162.4	118.5
$[MQI^{Me}]H$ (**2**)	CH_2Cl_2	8.93	3.43	6.75		135.3	162.2	116.1
$[MQI^{Me}]H$ (**2**)	THF	7.58	3.38	6.83		135.4	161.5	114.4
$[MQI^{Me}]H$ (**2**)	THF-d_8 + KH	7.58	3.34	6.68, 6.90	7.20	134.4, 136.1	161.3	112.0
$[MQI^{Me}]H$ (**2**)	C_6D_5Br	5.17	2.84	6.37	7.50	134.0	161.0	114.1
$[MQI^{Me}]H$ (**2**)	C_6D_5Br + KH	5.17	2.82	6.23, 6.50	7.73	133.0, 134.8	160.9	113.2
$[MQI^{Me}]H$ (**2**)	C_6D_6	2.27	2.26	6.16	8.07	134.1	161.4	112.8
$[MQI^{Me}]H$ (**2**)	C_6D_6 + KH	2.27	2.24	5.98, 6.32	8.12	133.2, 135.0	161.4	111.7
$[MQI^{tBu}]H$ (**3**)	C_6D_6	2.27	2.34	6.39		134.7	161.1	
$[MQI^{tBu}]H$ (**3**)	C_6D_6 + KH	2.27	2.21	6.07, 6.41	8.14	133.3, 135.0	161.6	111.5
$[MQI^{tBu}]H$ (**3**)	THF + KH	7.58	3.44	6.74, 6.92	7.21	134.1, 135.8	161.3	113.3
$[MQI^{Me}]H_2^+I^-$ (**6**)	THF	7.58	4.28	8.55	6.64			
$[MQI^{Me}]H_2^+I^-$ (**6**)	$CDCl_3$	4.81	3.95	7.80	5.82	140.3	152.6	161.1
$[MQI^{tBu}]H_2^+I^-$ (**7**)	DMSO-d_6	46.7	3.96	8.15	6.62	142.3	153.7	
$[MQI^{tBu}]H_2^+I^-$ (**7**)	CD_3CN	37.5	4.01	7.97	6.05	141.6	154.2	
$[MQI^{tBu}]H_2^+I^-$ (**7**)	THF	7.58	4.40	8.66	6.44	143.5	154.8	
$[MQI^{tBu}]H_2^+I^-$ (**7**)	$CDCl_3$	4.81	4.43	8.20	5.72	141.5	153.8	163.0
$[MQI^{tBu}]H_2^+I^-$ (**7**)	C_6D_6	2.27	1.55	8.19	4.01	142.1	153.1	

$[MQI^{tBu}]H_2^+Cl^-$ (**8**)	$CDCl_3$	4.81	4.48	8.31	5.74	142.0	153.7	164.3
$[MQI^{Me}]H \cdot AlMe_3$ (**9**)	C_6D_6	2.27	2.40	6.15, 6.31	6.52	136.3, 139.9	162.6	146.9
$[MQI^{tBu}]H \cdot AlMe_3$ (**10**)	C_6D_6	2.27	2.23	6.13, 6.19	6.51	136.2, 140.0	163.3	153.1
$[MQI^{Me}]H \cdot B(C_6F_5)_3$ (**11**)	C_6D_6	2.27	2.01	5.96, 6.17	7.00	135.8, 142.6	159.0	145.5
$\{[MQI^{tBu}]MgCl(THF)\}_2$ (**12**)	THF	7.58	3.32	6.61		135.3	165.2	110.1
$\{[MQI^{tBu}]MgCl(THF)\}_2$ (**12**)	C_6D_6	2.27	2.24	6.30		135.4	165.2	110.3
$\{[MQI^{tBu}]MgMe\}_2$ (**13**)	THF	7.58	3.25	6.50		134.6	162.0	105.4
$\{[MQI^{tBu}]MgMe\}_2$ (**13**)	C_6D_6	2.27	2.26	6.27		135.2	163.9	109.9
$\{[MQI^{tBu}]AlMe_2\}_2$ (**14**)	THF	7.58	3.44	6.77		136.7	165.5	122.4
$\{[MQI^{tBu}]ZnMe\}_2$ (**15**)	C_6D_6	2.27	2.23	6.22		135.5	162.2	111.8

Table 3. Summary of selected bonds lengths

	Bond length, Å				
Compound	1N-2C	2C-3C	3C-4C	4C-4N	4N-H or 4C-M
1·HX[55]	1.325(12)-1.375(4)	1.341(15)-1.366(5)	1.380(4)-1.436(4)	1.319(14)-1.367(5)	0.949(18)-1.15(3)
$[MQI^{tBu}]H_2^+Cl^-$ **8**	1.344(3)-1.351(3)	1.358(3)-1.371(3)	1.426(3)-1.430(3)	1.326(3)	0.87(4)-0.98(3)
1	1.357(2)-1.375(2)	1.339(3)-1.342(3)	1.422(3)-1.434(2)	1.305(2)-1.311(2)	0.99(3)-1.15(3)
$[MQI^{Me}]H$ (**2**)	1.360(2)	1.360(2)	1.466(2)	1.303(2)	0.94(2)
$[MQI^{tBu}]H$ (**3**)	1.3622(17)-1.3705(17)	1.3537(19)-1.3578(18)	1.4645(18)-1.4670(18)	1.3006(17)-1.3013(18)	0.92(2)-0.93(2)
$[MQI^{Me}]H \cdot B(C_6F_5)_3$ (**11**)	1.349(3)-1.350(3)	1.350(3)-1.367(3)	1.432(3)-1.452(3)	1.3333(3)	0.82(3) (NH), 1.566(3) (NB)
$\{[MQI^{Me}]MgCl(THF)\}_2$ (**16**)	1.363(3)-1.368(3)	1.357(3)-1.358(3)	1.491(3)-1.501(3)	1.282(2)	2.0537(17)- 2.0836(17)
$\{[MQI^{tBu}]MgCl(THF)\}_2$ (**12**)	1.368(2)-1.374(2)	1.350(2)-1.355(2)	1.480(2)-1.489(2)	1.281(2)	2.0498(15)-2.0713(14)
$\{[MQI^{tBu}]MgMe\}_2$ (**13**)	1.365(2)-1.371(2),	1.349(2)-1.360(2)	1.480(2)-1.485(2)	1.287(2)-1.288(2)	2.0470(16)-2.0549(16)
$\{[MQI^{tBu}]AlMe_2\}_2$ (**14**)	1.3662(13)	1.3620(14)-1.3641(14)	1.4711(13)-1.4726(13)	1.3023(12)	1.9408(9)-1.9412(8)
$\{[MQI^{tBu}]ZnMe\}_2$ (**15**)	1.358(3)-1.370(3)	1.355(3)-1.361(3)	1.474(3)-1.485(3)	1.285(3)-1.292(3)	1.9890(19)-2.0157(19)

Bond lengths give an alternate insight into the bonding in these compounds, and relevant bond lengths are summarized in Table 3.

From Table 3, it can be seen that 1N-2C and 2C-3C bonds are practically identical in pyridinium salts (**1·HX**[55] and **8**), pyridin-4(1H)-imines (**1-3**) and MQI-metal complexes. The 3C-4C bond has the same length for pyridinium salts and pyridin-4(1H)-imines, however for main group metal complexes it is significantly elongated. The most sensitive is 4C-4N bond length, which is the longest for pyridinium salts, with values typically for a single bond. In neutral NQAs this bond (1.300-1.311 Å) is still longer than a typical double C=N bond (1.251-1.291, by CCDC, where N was fixed to be two-coordinated). For the metal complexes reported here this bond was the shortest, like a typical double bond. For $[MQI^{Me}]H{\cdot}B(C_6F_5)_3$ (**11**) the bond lengths are similar to pyridinium salts, which supports a zwitterionic structure as proposed earlier. For $\{[MQI^{tBu}]AlMe_2\}_2$ (**14**) the 3C-4C bond is slightly shorter and the 4C-4N bond is slightly longer than for other metal complexes, implying that the Lewis acidic nature of Al which makes a contribution towards the zwitterionic structure of this compound; the same proposal was already made the NMR chemical shifts.

Conclusion. Novel monoanionic quasi-imide (MQI) ligands and their coordination compounds with main-group metals were synthesized and characterized. The ligand, structurally similar to imidazolin-2-imide and phosphoramide, has the potential to be a 6-electron donor like cyclopentadienide. It is especially efficient in positive charge delocalization because of resonance structures with aromatized pyridine ring. Both NMR shifts and bond lengths confirm this effect. These ligands may find applications to stabilize cationic and high oxidation state metal ions. Charge delocalization is likely for cationic early transition metals complexes with these ligands, and will be examined in future studies.

Experimental.

General Procedures. NMR spectroscopy was done using a Bruker Avance III instrument, 500 MHz for ^{1}H, 125 MHz for ^{13}C, 50.7 MHz for ^{15}N. Internal or external standards: tetramethylsilane for ^{1}H, ^{13}C, liquid NH_3 for ^{15}N (Bruker scale), $Et_2O{\cdot}BF_3$ for ^{11}B, $CFCl_3$ for ^{19}F. Mass spectra were measure using Waters MALDI Synapt G-2Si (for MALDI ionization) or Waters XEVO G2-XS (ESI, APCI or ASAP ionization) instruments. Elemental analysis was performed with PerkinElmer 2400 combustion CHN analyser. For filtration through silica, Silicycle SiliaFlash P60 silica gel R12030B (230-400 mesh, 40-63 µm particle size) was used. For dry column vacuum chromatography (DCVC)[56] and in other cases when mentioned Merck 1.15111 silica gel (Silica gel 60, 0.015-0.040 mm particle size) was used (the choice of the product with small grain size was essential for reproducible separation). Analytical TLC was performed on Silicycle SiliaPlate aluminum backed TLC plates TLA-R10011B-323, 200 µm layer thickness, with fluorescent indicator, the spots were visualized in UV light (254 nm). Preparative TLC was performed on Silicycle SiliaPlate glass backed TLC plates TLG-R10011B-353, 2000 µm layer thickness, with fluorescent indicator, the bands were visualized in UV light (254 nm). Titration of organometallic reagents with salicylic aldehyde phenylhydrazone was done in accordance with published procedure.[57] The compounds 4-amino-1-methylpyridinium iodide,[58] 3,5-dibromopyridin-4-amine,[59] (3,5-dimethylphenyl)boronic acid,[60] 3,5-bis(3,5-dimethylphenyl)pyridin-4-amine (**4**),[53] (3,5-di-*tert*-butylphenyl)boronic acid,[61] and Me_2Zn[62] were prepared based on existing syntheses. Full experimental details are given in the Supporting Information.

Crystallographic Data. Single crystal X-ray data were collected on a Bruker D8 VENTURE diffractometer equipped with PHOTON II CPAD detector using Mo Kα X-ray or Cu Kα radiation. The data were collected with APEX3[63] software; data reduction was performed using SAINT[64] and corrected for absorption using

SADABS,[65] all programs implemented in APEX3 suite.[63] The structures were solved by the intrinsic phasing method using SHELXT[66] or by dual-space method using SUPERFLIP,[67] then refined with the assistance of SHELXL[66] employing either ShelXle[68] or WinGX[69] as the graphic interface. Heavy atoms were refined anisotropically (hydrogen atoms were refined isotropically). The positions of NH hydrogen atoms in structure **1**, **2**, **3**, **8** and **11** were located in the electron density map, and their locations were refined. For all other hydrogen atoms a riding model was used, with the atoms placed in idealized positions. Finally the structures were visualized in Ortep3[69] program.

ASSOCIATED CONTENT

Supporting Information

Accession Codes

CCDC 2194594, 2194595, 2194903, 2194929, 2194941, 2194978, 2195231, 2195234, 2195246, 2195248 contain the supplementary crystallographic data for this paper. These data can be obtained free of charge via www.ccdc.cam. ac.uk/data_request/cif, or by emailing data_request@ccdc.cam.ac.uk, or by contacting The Cambridge Crystallographic Data Centre, 12 Union Road, Cambridge CB2 1EZ, UK; fax: +44 1223 336033.

Acknowledgement. S.A.J. acknowledges the Natural Sciences and Engineering Research Council (NSERC) of Canada for funding. We are grateful to Dr. Janeen Auld and Dr. Matthew James Revington for their help with mass spectrometry and NMR spectroscopy.

1. Gade, L. H., Taming early transition metals: the use of polydentate amido-donor ligands to create well defined reactive sites in reagents and catalysts. *Chem. Commun.* **2000**, 173-181.
2. Trambitas, A. G.; Panda, T. K.; Jenter, J.; Roesky, P. W.; Daniliuc, C.; Hrib, C. G.; Jones, P. G.; Tamm, M., Rare-Earth Metal Alkyl, Amido, and Cyclopentadienyl Complexes Supported by Imidazolin-2-iminato Ligands: Synthesis, Structural Characterization, and Catalytic Application. *Inorg. Chem.* **2010,** *49*, 2435-2446.
3. Trambitas, Alexandra G.; Panda, Tarun K.; Tamm, M., Rare Earth Metal Complexes Supported by Ancillary Imidazolin-2-iminato Ligands. *Z. Anorg. Allg. Chem.* **2010,** *636*, 2156-2171.
4. Hayes, C. E.; Leznoff, D. B., Actinide coordination and organometallic complexes with multidentate polyamido ligands. *Coordin. Chem. Rev.* **2014,** *266-267*, 155-170.
5. Lappert, M.; Protchenko, A.; Power, P.; Seeber, A., *Metal amide chemistry*. John Wiley & Sons2009; p 1 online resource (xii, 355 pages) : illustrations, plans.
6. Anwander, R., Lanthanide amides. In *Organolanthoid Chemistry: Synthesis, Structure, Catalysis*, Springer Berlin Heidelberg: Berlin, Heidelberg, 1996; pp 33-112.
7. Taillefer, M.; Rahier, N.; Minta, E.; Cristau, H.-J., New Applications of Ph 3 P=N--Li in Organic Synthesis and Heteroatom Chemistry. *Phosphorus Sulfur* **2002,** *177*, 1847-1850.

8. Ramos, A.; Stephan, D. W., Titanium ferrocenyl-phosphinimide complexes. *Dalton Trans.* **2010,** *39*, 1328-1338.
9. Winslow, C.; Lee, H. B.; Field, M. J.; Teat, S. J.; Rittle, J., Structure and Reactivity of a High-Spin, Nonheme Iron(III)- Superoxo Complex Supported by Phosphinimide Ligands. *J. Am. Chem. Soc.* **2021,** *143*, 13686-13693.
10. Lui, M. W.; Merten, C.; Ferguson, M. J.; McDonald, R.; Xu, Y.; Rivard, E., Contrasting Reactivities of Silicon and Germanium Complexes Supported by an N-Heterocyclic Guanidine Ligand. *Inorg. Chem.* **2015,** *54*, 2040-2049.
11. Peters, M.; Baabe, D.; Maekawa, M.; Bockfeld, D.; Zaretzke, M.-K.; Tamm, M.; Walter, M. D., Pogo-Stick Iron and Cobalt Complexes: Synthesis, Structures, and Magnetic Properties. *Inorg. Chem.* **2019,** *58*, 16475-16486.
12. Tamm, M.; Randoll, S.; Bannenberg, T.; Herdtweck, E., Titanium complexes with imidazolin-2-iminato ligands. *Chem. Commun.* **2004**, 876-877.
13. Tamm, M.; Randoll, S.; Herdtweck, E.; Kleigrewe, N.; Kehr, G.; Erker, G.; Rieger, B., Imidazolin-2-iminato titanium complexes: synthesis, structure and use in ethylene polymerization catalysis. *Dalton Trans.* **2006**, 459-467.
14. Shoken, D.; Sharma, M.; Botoshansky, M.; Tamm, M.; Eisen, M. S., Mono(imidazolin-2-iminato) Titanium Complexes for Ethylene Polymerization at Low Amounts of Methylaluminoxane. *J. Am. Chem. Soc.* **2013,** *135*, 12592-12595.
15. Shoken, D.; Shimon, L. J. W.; Tamm, M.; Eisen, M. S., Synthesis of Imidazolin-2-iminato Titanium Complexes Containing Aryloxo Ligands and Their Catalytic Performance in the Polymerization of α-Olefins. *Organometallics* **2016,** *35*, 1125-1131.
16. Lysenko, S.; Daniliuc, C. G.; Jones, P. G.; Tamm, M., Tungsten alkylidyne complexes with ancillary imidazolin-2-iminato and imidazolidin-2-iminato ligands and their use in catalytic alkyne metathesis. *J. Organomet. Chem.* **2013,** *744*, 7-14.
17. Bunquin, J. C.; Stryker, J. M. Transition metal-phosphoranimide catalysts. CA2799352A1, 2014.
18. Nomura, K.; Patamma, S.; Matsuda, H.; Katao, S.; Tsutsumi, K.; Fukuda, H., Synthesis of half-titanocenes containing 1,3-imidazolidin-2-iminato ligands of type, Cp*TiCl2[1,3-R2(CH2N)2C[double bond, length as m-dash]N]: highly active catalyst precursors in ethylene (co)polymerisation. *RSC Adv.* **2015,** *5*, 64503-64513.
19. Karmel, I. S. R.; Khononov, M.; Tamm, M.; Eisen, M. S., Uranium-mediated ring-opening polymerization of ?-caprolactone: a comparative study. *Cat. Sci.Technol.* **2015,** *5*, 5110-5119.
20. Wu, X.; Tamm, M., Transition metal complexes supported by highly basic imidazolin-2-iminato and imidazolin-2-imine N-donor ligands. *Coordin. Chem. Rev.* **2014,** *260*, 116-138.
21. Dehnicke, K.; Strähle, J., Phosphorane iminato complexes of transition metals. *Polyhedron* **1989,** *8*, 707-726.
22. Doster, M. E.; Hatnean, J. A.; Jeftic, T.; Modi, S.; Johnson, S. A., Catalytic C-H Bond Stannylation: A New Regioselective Pathway to C-Sn Bonds via C-H Bond Functionalization. *J. Am. Chem. Soc.* **2010,** *132*, 11923-11925.
23. Doster, M. E.; Johnson, S. A., Selective C-F bond activation of tetrafluorobenzenes by nickel(0) with a nitrogen donor analogous to H-heterocyclic carbenes. *Angew. Chem., Int. Ed.* **2009,** *48*, 2185-2187.
24. Doster, M. E.; Johnson, S. A., Carbon-hydrogen bond stannylation and alkylation catalyzed by nitrogen-donor-supported nickel complexes: intermediates with Ni-Sn bonds and catalytic carbostannylation of ethylene with organostannanes. *Organometallics* **2013,** *32*, 4174-4184.
25. Johnson, S. A.; Doster, M. E.; Hatnean, J. A. Regioselective catalytic conversion of hydrocarbons to versatile synthetic reagents via C-H bond functionalization. US20110282087A1, 2011.
26. Shi, Q.; Thatcher, R. J.; Slattery, J.; Sauari, P. S.; Whitwood, A. C.; McGowan, P. C.; Douthwaite, R. E., Synthesis, Coordination Chemistry and Bonding of Strong N-Donor Ligands Incorporating the 1H-Pyridin-(2E)-Ylidene (PYE) Motif. *Chem. Eur. J.* **2009,** *15*, 11346-11360.
27. Sahin, C.; VarlikII, C.; Zafer, C.; Shi, Q.; Douthwaite, R. E., A new 1H-pyridin-(2E)-ylidene ruthenium complex as sensitizer for a dye-sensitized solar cell. *J. Coord. Chem.* **2013,** *66*, 1384-1395.

28. Abdolla, N. S. Y.; Davies, D. L.; Singh, K., Bis-Cyclometallated Iridium(III) Complexes with Bidentate Ligands Containing One or Two Pyridylideneamine (PYE) Donors: Influence of PYE Substitution (para or ortho) on Complexation. *Eur. J. Inorg. Chem.* **2021,** *2021*, 939-950.
29. Thatcher, R. J.; Johnson, D. G.; Slattery, J. M.; Douthwaite, R. E., Charged Behaviour from Neutral Ligands: Synthesis and Properties of N-Heterocyclic Pseudo-amides. *Chem. Eur. J.* **2012,** *18*, 4329-4336.
30. Munir, N.; Masood, S.; Liaqat, F.; Tahir, M. N.; Yousuf, S.; Kalsoom, S.; Mughal, E. U.; Sumrra, S. H.; Maalik, A.; Zafar, M. N., Synthesis of new Pro-PYE ligands as co-catalysts toward Pd-catalyzed Heck–Mizoroki cross coupling reactions. *RSC Adv.* **2019,** *9*, 37986-38000.
31. Leigh, V.; Carleton, D. J.; Olguin, J.; Mueller-Bunz, H.; Wright, L. J.; Albrecht, M., Solvent-Dependent Switch of Ligand Donor Ability and Catalytic Activity of Ruthenium(II) Complexes Containing Pyridinylidene Amide (PYA) N-Heterocyclic Carbene Hybrid Ligands. *Inorg. Chem.* **2014,** *53*, 8054-8060.
32. Donnelly, K. F.; Segarra, C.; Shao, L.-X.; Suen, R.; Müller-Bunz, H.; Albrecht, M., Adaptive N-Mesoionic Ligands Anchored to a Triazolylidene for Ruthenium-Mediated (De)Hydrogenation Catalysis. *Organometallics* **2015,** *34*, 4076-4084.
33. Salzmann, K.; Segarra, C.; Albrecht, M., Donor-Flexible Bis(pyridylidene amide) Ligands for Highly Efficient Ruthenium-Catalyzed Olefin Oxidation. *Angew. Chem., Int. Ed.* **2020,** *59*, 8932-8936.
34. Navarro, M.; Segarra, C.; Pfister, T.; Albrecht, M., Structural, Electronic, and Catalytic Modulation of Chelating Pyridylideneamide Ruthenium(II) Complexes. *Organometallics* **2020,** *39*, 2383-2391.
35. Navarro, M.; Smith, C. A.; Albrecht, M., Enhanced Catalytic Activity of Iridium(III) Complexes by Facile Modification of C,N-Bidentate Chelating Pyridylideneamide Ligands. *Inorg. Chem.* **2017,** *56*, 11688-11701.
36. Navarro, M.; Li, M.; Müller-Bunz, H.; Bernhard, S.; Albrecht, M., Donor-Flexible Nitrogen Ligands for Efficient Iridium-Catalyzed Water Oxidation Catalysis. *Chem. Eur. J.* **2016,** *22*, 6740-6745.
37. Navarro, M.; Li, M.; Bernhard, S.; Albrecht, M., A mesoionic nitrogen-donor ligand: structure, iridium coordination, and catalytic effects. *Dalton Trans.* **2018,** *47*, 659-662.
38. Koenigs, E.; Friedrich, H.; Jurany, h., Über einige Derivate des 4-Amino-pyridins. *Chem. Ber.* **1925,** *58*, 2571-2576.
39. Tschitschibabin, A. E.; Ossetrowa, E. D., Zur Tautomerie des γ-Amino-pyridins. II. Mitteilung über methzlierte Derivate des γ-Amino-pyridins. *Chem. Ber.* **1925,** *58*, 1708-1712.
40. Angyal, S. J.; Angyal, C. L., The Tautomerism of N-Hetero-aromatic Amines. Part I. *J. Chem. Soc.* **1952**, 1461-1466.
41. Anderson, L. C.; Seeger, N. V., The Absorption Spectra of the Aminopyridines. *J. Am. Chem. Soc.* **1949,** *71*, 340-342.
42. Angyal, C. L.; Werner, R. L., The Tautomerism of N-Heteroaromatic Amines. Part II. Infra-red Spectroscopic Evidence. *Journal of the Chemical Society* **1952**, 2911-2915.
43. Grønneberg, T., Mass Spectrometry of Methylaminopyridines and Their Quaternary Salts. *Chemica Scripta* **1973,** *3*, 139-141.
44. Grønneberg, T.; Undheim, K., Mass Spectrometry of Onium Compounds - XV. Ionization Potentials of Amino Pyridines. *Tetrahedron Lett.* **1972,** *13*, 3193-3196.
45. Stefaniak, L., ^{14}N and ^{13}C NMR of Tautomeric Systems of Mercapto- and Amino-pyridines. *Org. Magn. Resonance* **1979,** *12*, 379-382.
46. Batts, B. D.; Spinner, E., Vibration-Spectral and Structural Comparison of the 4-Aminopyridine Cations with the 4-Hydroxypyridinium Ion and 4-Pyridone. The Protio Parent Ions, N- and C-Deuterated, and N-Methylated Ions. Relevant N.M.R. Spectral Studies. *Austr. J. Chem.* **1969,** *22*, 2595-2610.
47. Cook, M. J.; Katritzky, A. R.; Linda, P.; Tack, R. D., Aromaticity and tautomerism. Part II. The 4-pyridone, 2-quinolone, and 1-isoquinolone series. *J. Chem. Soc., Perkin Trans. 2* **1973**, 1080-1086.
48. Alexandrou, N. E.; Soulis, T. P., Identification of Isomeric Dihydro-Azines by Benzene Induced Shifts in NMR Spectra. VI. *Tetrahedron Lett.* **1972**, 1417-1419.
49. Foye, W. O.; Kay, D. H., Antiradiation compounds. IX. Dithiocarbamates of strongly basic pyridines and pyrimidines. *J. Pharm. Sci.* **1968,** *57*, 345-348.
50. Rokach, J.; Hamel, P.; Hunter, N. R.; Reader, G.; Rooney, C. S.; Anderson, P. S.; Cragoe Jr, E. J.; Mandel, L. R., Cyclic amidine inhibitors of indolamine N-methyltransferase. *J. Med. Chem.* **1979,** *22*, 237-247.

51. Lambert, C.; Gaschler, W.; Zabel, M.; Matschiner, R.; Wortmann, R., Linear and non-linear optical properties of arene-Fe-Cp complexes. *J. Organomet. Chem.* **1999,** *592*, 109 - 114.
52. Acheson, R. M.; Woollard, J., Addition Reactions of Heterocyclic Compounds. Part LXI. Reactions of Electrophilic Acetylenes with Conjugated Cyclic Enamines. *J. Chem. Soc., Perkin Trans. 1* **1975**, 744 - 748.
53. Ashikawa, M.; Nishiyama, T. Bisphenylpyridine compounds, and erythropoietin production promoters and anemia treatment agents containing them. JP2011063565A, 2011.
54. Patroni, J.; Skelton, B.; Stick, R.; White, R., The reaction of methyl 4,6-O-isopropylidene-2,3-O-thiocarbonyl-α-D-mannoside with methyl iodide : a synthesis of methyl α-Tyveloside (methyl 3,6-dideoxy-α-D-*arabino*-hexopyranoside). *Aust. J. Chemistry* **1980,** *33*, 987-999.
55. Anwar; Okada, S.; Oikawa, H.; Nakanishi, H., Preparation and Crystal Structures of New Colorless 4-Amino-1-methylpyridinium Benzenesulfonate Salts for Second-Order Nonlinear Optics. *Chem. Mater.* **2000,** *12*, 1162-1170.
56. Pedersen, D. S.; Rosenbohm, C., Dry Column Vacuum Chromatography. *Synthesis* **2001,** *2001*, 2431-2434.
57. Love, B. E.; Jones, E. G., The Use of Salicylaldehyde Phenylhydrazone as an Indicator for the Titration of Organometallic Reagents. *J. Org. Chem.* **1999,** *64*, 3755-3756.
58. Krzyżaniak, A.; Leeman, M.; Vossebeld, F.; Visser, T. J.; Schuur, B.; de Haan, A. B., Novel extractants for the recovery of fermentation derived lactic acid. *Sep. Purif. Technol.* **2013,** *111*, 82-89.
59. Cañibano, V.; Rodríguez, J. F.; Santos, M.; Sanz-Tejedor, M. A.; Carreño, M. C.; González, G.; García-Ruano, J. L., Mild Regioselective Halogenation of Activated Pyridines with N-Bromosuccinimide. *Synthesis* **2001,** *2001*, 2175-2179.
60. Lin, X.; Telepeni, I.; Blake, A. J.; Dailly, A.; Brown, C. M.; Simmons, J. M.; Zoppi, M.; Walker, G. S.; Thomas, K. M.; Mays, T. J.; Hubberstey, P.; Champness, N. R.; Schröder, M., High Capacity Hydrogen Adsorption in Cu(II) Tetracarboxylate Framework Materials: The Role of Pore Size, Ligand Functionalization, and Exposed Metal Sites. *J. Am. Chem. Soc.* **2009,** *131*, 2159-2171.
61. Schöbel, A.; Herdtweck, E.; Parkinson, M.; Rieger, B., Ultra-Rigid Metallocenes for Highly Iso- and Regiospecific Polymerization of Propene: The Search for the Perfect Polypropylene Helix. *Chem. Eur. J.* **2012,** *18*, 4174-4178.
62. Eremeev, I. V.; Danov, S. M.; Skudin, A. G.; Sakhipov, V. R., Preparation of Organozinc and Organocadmium Compounds from the Metals and Alkyl Halides in the Presence of Stimulating Systems Based on a Derivative a Transition Metal and an Organometallic Compound. *Russian J. Gen. Chem.* **2003,** *73*, 556-559.
63. *APEX3*, Bruker AXS Inc.: Madison, WI, 2016.
64. *SAINTPlus*, Bruker AXS Inc.: Madison, WI, 2012.
65. *SADABS*, Bruker AXS Inc.: Madison, WI, 2012.
66. Sheldrick, G., SHELXT - Integrated space-group and crystal-structure determination. *Acta Crystallogr. A* **2015,** *71*, 3-8.
67. Palatinus, L.; Chapuis, G., SUPERFLIP - a computer program for the solution of crystal structures by charge flipping in arbitrary dimensions. *J. Appl. Crystallogr.* **2007,** *40*, 786-790.
68. Hubschle, C. B.; Sheldrick, G. M.; Dittrich, B., ShelXle: a Qt graphical user interface for SHELXL. *J. Appl. Crystallogr.* **2011,** *44*, 1281-1284.
69. Farrugia, L., WinGX and ORTEP for Windows: an update. *J. Appl. Crystallogr.* **2012,** *45*, 849-854.